Electronic origin of half-metal to semiconductor transition and colossal magnetoresistance in spinel $HgCr_2Se_4$

Aiji Liang,[1,2,3,*] Zhilin Li,[4,*] Shihao Zhang,[1,2,*] Shucui Sun,[5] Shuai Liu,[1] Cheng Chen,[1,2,3,6] Haifeng Yang,[1] Shengtao Cui,[1] Sung-Kwan Mo,[3] Shuai Yang,[4] Yongqing Li,[4] Meixiao Wang,[1,2] Lexian Yang,[5] Jianpeng Liu,[1,2,†] Zhongkai Liu,[1,2,‡] and Yulin Chen[1,2,5,6,§]

[1]*School of Physical Science and Technology, ShanghaiTech University, Shanghai, People's Republic of China*
[2]*ShanghaiTech Laboratory for Topological Physics, Shanghai 200031, People's Republic of China*
[3]*Advanced Light Source, Lawrence Berkeley National Laboratory, Berkeley, California 94720, USA*
[4]*Beijing National Laboratory for Condensed Matter Physics Institute of Physics, Chinese Academy of Sciences, Beijing 100190, China*
[5]*State Key Laboratory of Low Dimensional Quantum Physics, Department of Physics and Collaborative Innovation Center of Quantum Matter, Tsinghua University, Beijing 100084, People's Republic of China*
[6]*Department of Physics, University of Oxford, Oxford OX1 3PU, United Kingdom*

(Received 22 September 2022; revised 12 February 2023; accepted 4 April 2023; published 9 May 2023)

Half metals are ferromagnets hosting spin-polarized conducting carriers and are crucial for spintronics applications. The chromium spinel $HgCr_2Se_4$ represents a unique type of half-metal, which features a half-metal to semiconductor transition (HMST) and exhibits colossal magnetoresistance (CMR) across the ferromagnetic-paramagnetic (FM-PM) transition. Using angle-resolved photoemission spectroscopy, we find that the Fermi surface of *n*-type $HgCr_2Se_4$ (*n*-$HgCr_2Se_4$) consists of a single electron pocket which moves above the Fermi level (E_F) upon the FM-PM transition, leading to the HMST. Such a Lifshitz transition manifests a giant band splitting which originates from the exchange interaction unveiled with a specific chemical nonstoichiometry. The exchange band splitting and the chemical nonstoichiometry are two key ingredients to the HMST and CMR, consistent with our *ab initio* calculation. Our findings provide spectroscopic evidence of the electronic origin of the anomalous properties of $HgCr_2Se_4$, which address the unique phase transition in half-metals.

DOI: 10.1103/PhysRevB.107.195114

I. INTRODUCTION

The interplay of the spin, charge, orbital, and lattice degrees of freedom in condensed matter provides important physical properties such as unconventional superconductivity [1], metal insulator transition [2], colossal magnetoresistance (CMR) [3], and the anomalous Hall effect [4]. First proposed in the 1980s, the half-metal is considered one such intriguing system [5]. A perfect half-metal hosts fully spin polarized conducting charge carriers that are ideal for spintronics applications. In the past decades, a handful of half-metals have been proposed, such as oxides [6–9] (e.g., CrO_2 [7]), spinels [9,10] (e.g., Fe_3O_4 [9]), perovskites [11,12] [e.g., (La, Sr)MnO_3 [3,11]], Heuslers [5,13,14] (e.g., NiMnSb [5]), and zinc blendes (e.g., CrAs [15]). Among them only few are experimentally verified to be half-metal with nearly 100% spin polarization [7,11].

Recently, the Cr-based chalcogenide spinel $HgCr_2Se_4$ has been theoretically proposed [16,17] and experimentally verified as a half-metal [18]. It possesses magnetic moments of $3\mu_B/Cr^{3+}$ with a spin polarization of the conducting carriers up to 97% [18]. Similar to mixed-valence manganites [3,19,20] and Eu-based chalcogenides [21–23], $HgCr_2Se_4$ shows an intriguing resistivity anomaly across the ferromagnetic-paramagnetic (FM-PM) transition, where the resistivity changes by several orders in magnitude, featuring a half-metal to semiconductor transition (HMST) [18,24–28]. The CMR [24,25,27] is observed in the same temperature regime as HMST (~20 K above and below T_C [25]). Moreover, $HgCr_2Se_4$ also hosts spiral-like antiferromagnetic insulating state under high pressure [29], $\sqrt{T}$-type dependence of versatile transport coefficients at low temperature [30], and may realize a Chern semimetal state [16] and other topological nontrivial states [17,31–34]. These unique properties make $HgCr_2Se_4$ an important platform to investigate the interplay between the half-metallicity, magnetism, and topology.

Despite the strong motivations, the electronic origin of the HMST, CMR, and other intriguing properties [35,36] in $HgCr_2Se_4$ remains elusive. Further, the proposed topologically nontrivial band structure [16,17] requires experimental verification. Nonetheless, the photoemission spectroscopy investigation on the electronic structure of $HgCr_2Se_4$ has not been achieved. Hence, a direct measurement of the electronic band structure would offer crucial evidence in answering these questions.

In this work, using angle-resolved photoemission spectroscopy (ARPES), we report a comprehensive electronic

*These authors contributed equally to this work.
†Corresponding author: liujp@shanghaitech.edu.cn
‡Corresponding author: liuzhk@shanghaitech.edu.cn
§Corresponding author: yulin.chen@physics.ox.ac.uk

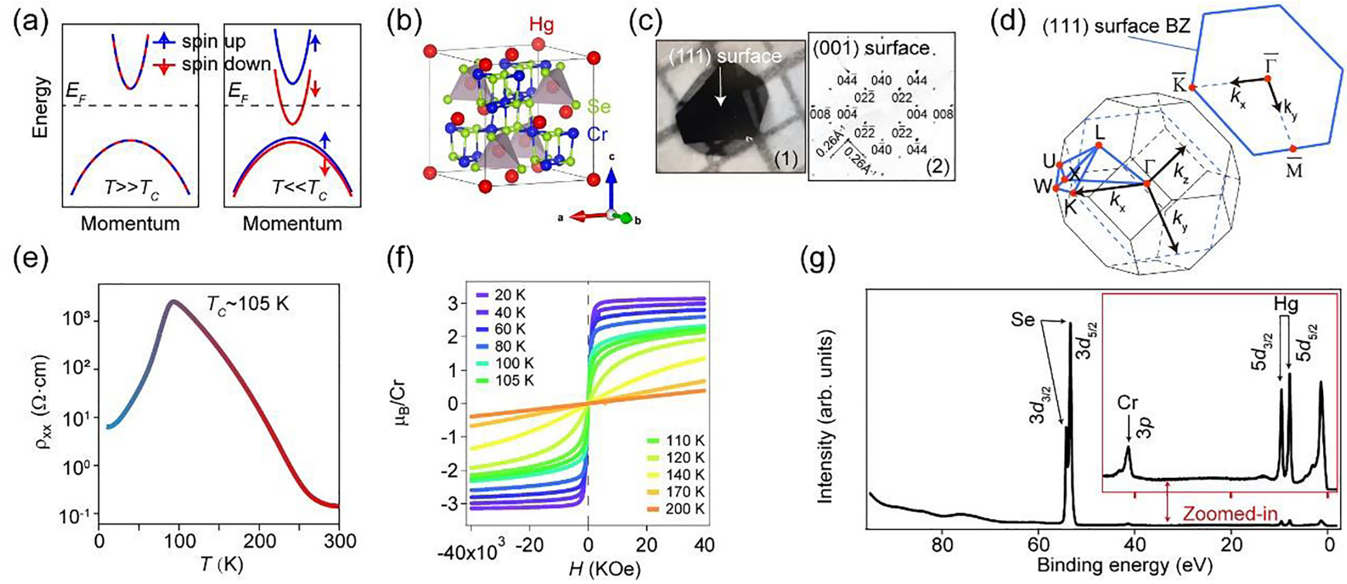

FIG. 1. Basic information and characterization of n-$HgCr_2Se_4$. (a) Schematic of band structure of n-$HgCr_2Se_4$ in the PM and FM states. (b) Crystal structure. (c) (1) Typical picture of the sample. The natural facet is the (111) surface. (2) Single crystal x-ray diffraction pattern. (d) Bulk BZ and (111) surface projected BZ. (e) Temperature dependent resistivity. (f) Temperature dependent magnetization across T_C. (g) XPS spectrum with sharp Se 3d, Cr 3p, and Hg 5d core levels.

structure study on n-$HgCr_2Se_4$. Far below T_C, we observed a Fermi surface produced by a single conduction band (CB) [17] and a characteristic ~0.3 eV direct band gap. Upon increasing temperature, the CB moves towards Fermi level (E_F) and eventually above it above T_C, showing a Lifshitz transition. Meanwhile the valence band (VB) remains almost unshifted, resulting in an increase of the band gap. Such an electronic evolution could be well reproduced by our *ab initio* calculations, which suggests the shift of CB is driven by the exchange interaction that splits bands. The resulting CB is thus fully spin polarized below T_C. Our findings reveal that the Lifshitz transition which can be tuned by both the chemical nonstoichiometry (E_F position) and the magnetic-field-mediated exchange band splitting are responsible for the ideal HMST [Fig. 1(a)] and CMR near T_C. These findings reveal the electronic origin of the most unusual properties in $HgCr_2Se_4$ and can be applied to related half-metals.

II. METHODS

ARPES measurements were performed at BL 10.0.1, BL 7.0.2, and BL 4.0.3 of the Advanced Light Source and BL 5-2 of the Stanford Synchrotron Radiation Light Source. BL 10.0.1 and BL 4.0.3 are equipped with R4000 analyzers. BL 7.0.2 and BL 5-2 are equipped with DA30 analyzers. The measured sample temperature and vacuum level were 20–250 K and lower than 5.0×10^{-11} Torr. The angle resolution was 0.2° and the overall energy resolution was better than 20 meV. Single crystals of n-$HgCr_2Se_4$ were grown by vapor transport method [30]. The Curie temperature T_C is ~105 K with the electron density in a range 10^{16}–10^{18} cm^{-3} [30]. All the calculations were generated by PBE + U (Perdew-Burke-Ernzerhof + U) method, with a Coulomb energy U on the Cr element of 5.5 eV.

III. RESULTS

$HgCr_2Se_4$ crystallizes in the space group $Fd3m$ [Fig. 1(b)]. The increase of the lattice by Se makes the FM Cr-Se-Cr interaction prevail the Cr-Cr antiferromagnetic interaction [37], resulting in a FM transition at ~105 K [18,28,30]. High quality samples [Fig. 1(c1)] have an octahedral shape, flat shining surfaces, and sharp edges with sharp Bragg peaks [Fig. 1(c2)] and core levels [Fig. 1(g)]. Figure 1(d) shows the bulk and projected (111) surface Brillouin zones (BZs). The n-type nature (the as-grown sample is moderately n doped [25]) is confirmed by Hall resistivity measurements [38,39]. The temperature dependent resistivity indicates a FM-PM transition at ~105 K with a resistivity variation by several orders in magnitude [Fig. 1(e)]. Below T_C, the magnetization shows clear soft ferromagnetism [(Fig. 1(f)]. Above T_C, the magnetization curves gradually approach the linear shape, suggesting strong FM fluctuations above T_C. The saturated magnetization at low temperature (20 K) under the assumption of stoichiometry is slightly larger than the expected saturation of $3\mu_B/Cr^{3+}$ [18]. This may be caused by several reasons, for example, the mass measuring difference or the chemical nonstoichiometry (mainly Hg and Se vacancies) [25].

The band structure of n-$HgCr_2Se_4$ in the FM state on the (111) surface is illustrated in Fig. 2. The freshly cleaved surface is slightly less n doped compared to the as-grown surface because of the rich interior Hg vacancies [25] (see Supplemental Material Fig. S1 [40]). Therefore, the photoemission spectrum observed on the as-cleaved samples only contain holelike bands [Figs. 2(a)–2(c)]. The constant energy contour

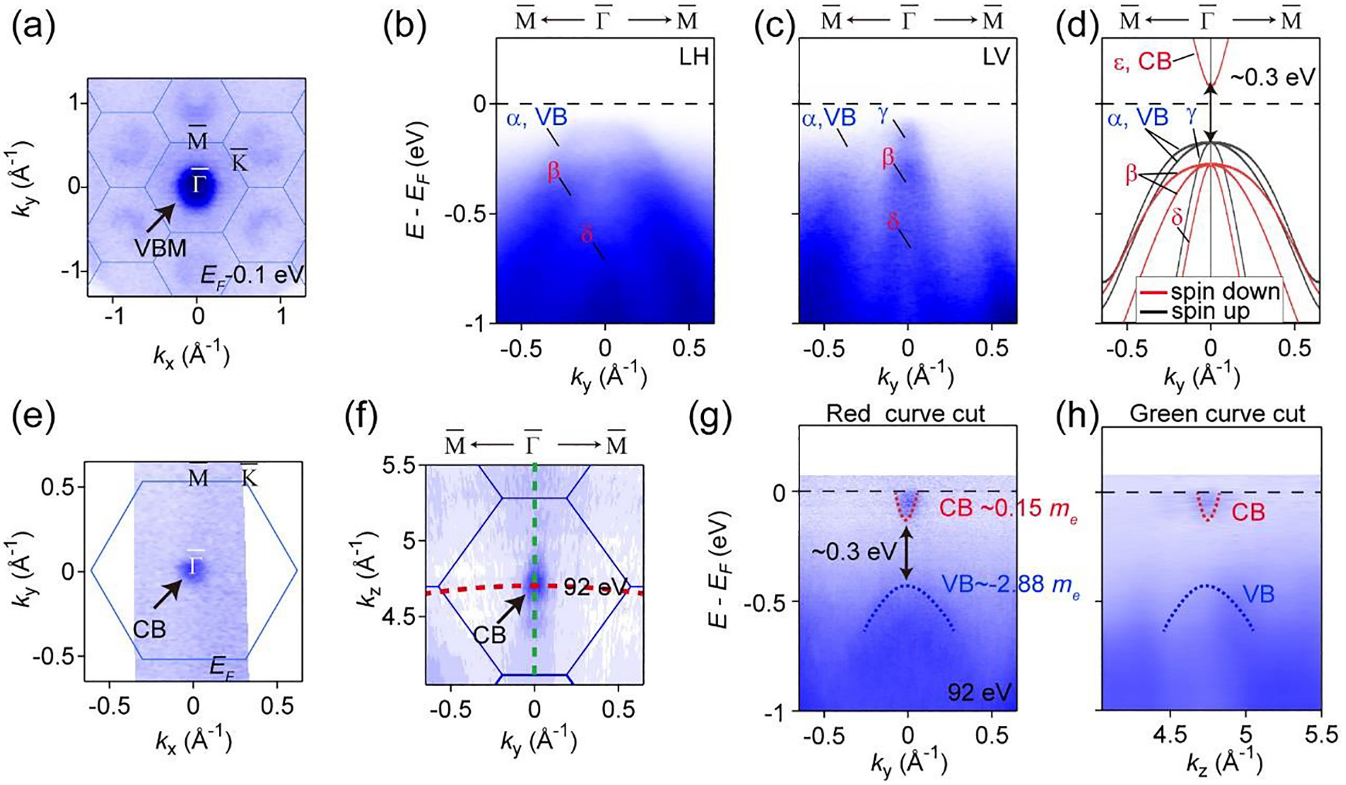

FIG. 2. Basic band structure of n-$HgCr_2Se_4$ on the (111) surface in the FM state. (a) CEC which cuts through the VB maximum (VBM). (b),(c) Band dispersions along $\bar{\Gamma}$-$\bar{M}$ measured by LH and LV photons. (d) Calculated spin-resolved bands along $\bar{\Gamma}$-$\bar{M}$. The bands (α, β, γ, δ, ε) are denoted accordingly. (e) CEC near E_F after K deposition in the k_x-k_y plane. (f) CEC near E_F after K deposition in the k_y-k_z plane. (g),(h) Extracted bands along the red and green momentum curves in (f). The spectrum in (g) and (h) is normalized by dividing momentum-integrated EDC along the momentum direction. The measured temperature is $\sim$20 K.

(CEC) near the VB maximum shows a clear sixfold symmetry, consistent with the (111) surface cleavage [Fig. 2(a)]. By using both the linear horizontal (LH) and vertical (LV) polarized photons, four sets of holelike bands (α, β, γ, δ) along $\bar{\Gamma}$-$\bar{M}$ [Figs. 2(b) and 2(c)] are identified, agreeing well with the calculation [Fig. 2(d)].

To measure the band structure of the CB, we raise the E_F by using *in situ* surface alkaline metal (K) deposition (see Supplemental Material Fig. S2 [40]). Upon K doping, the CB [ε band, a small electron pocket at $\bar{\Gamma}$ as labeled in Fig. 2(d)] appears below E_F [Figs. 2(e)–2(h)]. Along the $\bar{\Gamma}$-$\bar{M}$ direction, the CB and VB (uppermost α band) have effective masses of 0.15 m_e and 2.88 m_e, and a $\sim$0.3 eV direct band gap at 20 K [Fig. 2(g)]. The CB and VB around $\bar{\Gamma}$ can also be observed by spectrum on the (001) cleaved surface (see Supplemental Material Fig. S3 [40]). By extracting the band dispersion along Γ-L [Fig. 2(h)], we further confirm there is no in-gap state. All the observed bands (α, β, γ, δ, ε) and the gap size are captured by our first-principle calculation [Fig. 2(d)]. From the calculations we conclude that the α, γ and β, δ bands are spin-split pairs in the FM state. Since the calculated spin splitting of the CB is $\sim$1 eV [16,17,37], the observed ε band is thus fully spin polarized (its spin split counterpart lies way above E_F), consistent with the half-metal nature in n-$HgCr_2Se_4$ [18]. Besides the Andreev reflection measurement [18], it would be great to show the spin polarization of the CB by other spin-resolved measurements in the future, such as spin-resolved ARPES.

We estimate the evolution of the CB, VB, and the band gap across T_C by temperature dependent measurement (see Fig. 3 and Supplemental Material Fig. S4 [40]). The CB spectrum, energy distribution curves (EDCs) at $\bar{\Gamma}$, and the normalized EDCs (with respect to the EDC at 105 K) are plotted in Figs. 3(a)–3(c), respectively. Figure 3(d) illustrates the temperature dependent CB bottom below T_C. The CB moves continuously towards E_F and disappears upon increasing temperature, suggesting a Lifshitz transition in the band structure. The abrupt change appears at 100–105 K [Figs. 3(a9) and 3(a10)] near T_C, where the CB disappears. Such an evolution is an intrinsic property of n-$HgCr_2Se_4$ since the CB would reappear below E_F after cycling the temperature back to 20 K [Fig. 3(a12)]. Contrarily, negligible changes are found in the VB upon temperature variation (see Supplemental Material Fig. S4 [40]).

Above T_C, there seems to be no density of states near E_F [Figs. 3(a10) and 3(a11)] in contrast to the observed electron pocket near E_F below T_C [Figs. 3(a1)–3(a8)]. Such an evolution of the Fermi surface could be explained by considering the impurity bands from Hg and Se vacancies. Our *ab initio* calculations demonstrate that the impurity bands from the Se vacancies lie across the CB bottom in the FM state [Fig. 3(e)]. When the CB moves upward in the PM state, the impurity

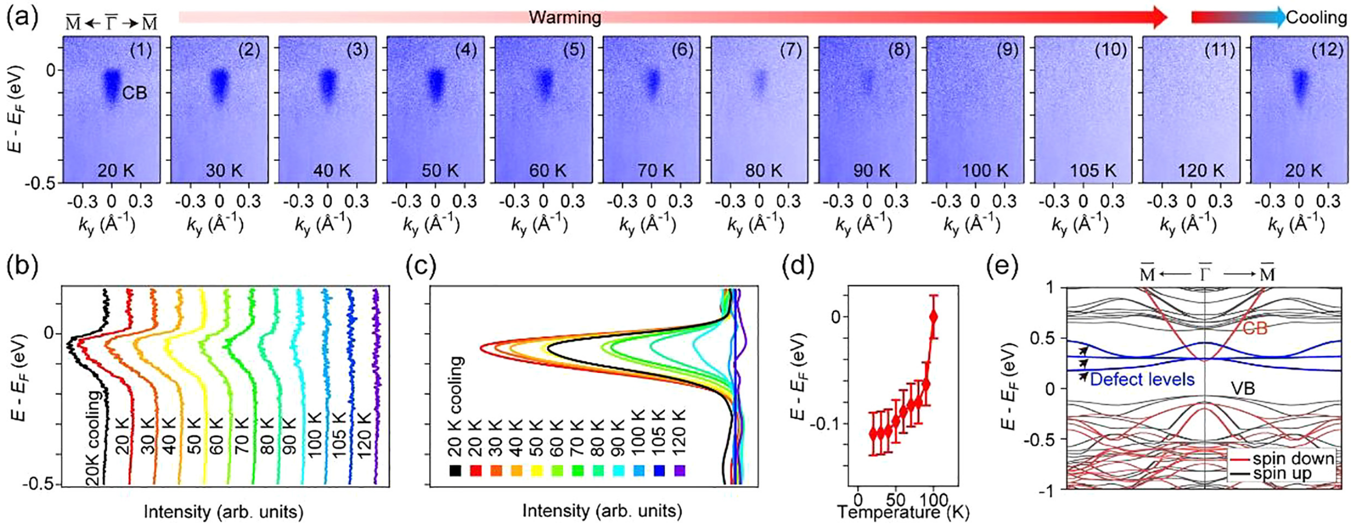

FIG. 3. Half-metal driven by ferromagnetism in n-$HgCr_2Se_4$. (a) Evolution of bands along $\bar{\Gamma}$-$\bar{M}$ after K doping at different temperatures. They are normalized in the same way as in Figs. 2(g) and 2(h). (b) Extracted temperature dependent EDCs from (a) with a momentum integration of ± 0.025 Å^{-1}. (c) Overlaid temperature dependent EDCs from (b). They are divided by the EDC at the temperature of 105 K. (d) The temperature dependent band bottom of the CB extracted from (a) and (b). (e) The spin-resolved band structure from the $Hg_{15}Cr_{32}Se_{63}$ supercell (Hg vacancy level is 1/16 and Se vacancy level is 1/64) which has defect levels from Hg and Se vacancies. The ones labeled by the blue color are mainly from the Se vacancies.

bands [41] lie within the band gap and accommodates the electrons from the CB. In return the impurity bands pin the E_F, leading to the observed band structure above T_C (see Supplemental Material Fig. S4 [40]). The electrons are transferred back to the CB from the impurity bands when the CB moves downward to cross the impurities bands in the FM state.

IV. DISCUSSION AND CONCLUSION

We summarize our temperature dependent results in Fig. 4(a). The disappearance of the CB across T_C in n-$HgCr_2Se_4$ suggests the band shift is associated with the ferromagnetism, which splits the CB via exchange interaction. On the other hand, the VB is not significantly affected by the ferromagnetism, *most likely due to its orbital characters*. The VB contains mostly Se p orbitals, which have small Coulomb energy U and thus much smaller band splitting than the CB with more Cr d orbitals [16,17,37] (see Supplemental Material Fig. S5 [40]).

The observed Lifshitz transition across the FM-PM transition provides the electronic origin of the HMST as well as the CMR, as summarized in Fig. 4(b). The transfer of electrons between localized impurities bands and the itinerant CB well accounts for the large variation in the resistivity in the HMST

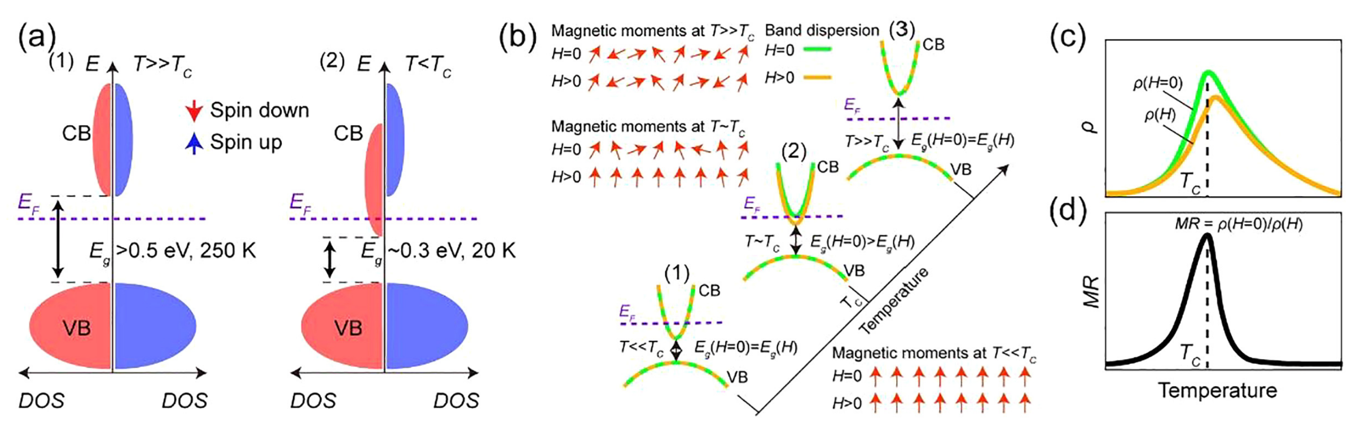

FIG. 4. Electronic origin of the HMST and CMR in n-$HgCr_2Se_4$. (a) Schematic of the electronic origin of the HMST. (1) $T < T_C$; the CB and VB have no spin related splitting. The band gap (E_g) is >0.5 eV at 250 K. (2) $T < T_C$; the CB splits and crosses E_F while the VB has minor changes. The band gap narrows to ~ 0.3 eV at 20 K. (b) Schematic of the electronic origin of the CMR. (1)–(3) Temperature dependent band structure with and without magnetic field at (1) $T \ll T_C$, (2) $T \sim T_C$, and (3) $T \gg T_C$. Inset: schematic of the alignment of the magnetic moments by magnetic field across T_C. (c) Schematic of the temperature dependent resistivity curve (ρ-T) of the HMST according to the electronic evolution in (b). (d) Schematic of the temperature dependent magnetoresistance showing CMR based on the ρ-T curve in (c). Note that the E_F position here is chosen according to the experimental observations in Fig. 3.

across T_C. Meanwhile, the external magnetic field aligns fluctuated spin moments near T_C [inset in Fig. 4(b)] [25,36,37]. The exchange splitting strength is thus tuned, leading to a magnetic field driven Lifshitz transition [Fig. 4(b2)] and the HMST [Fig. 4(c)], thereby achieving the CMR [Fig. 4(d)]. Such a mechanism from the electronic structure point of view may be much simplified (e.g., neglecting the defects scattering and the magnetic polarons [27,28,42,43]), however, it captures the essential physics. With different E_F positions due to different impurity levels, the HMST and CMR would change accordingly, also showing nice agreement with our interpretations (see Supplemental Material Fig. S6 [40]). The mechanism can also nicely explain the giant redshift of the optical absorption edge [35].

The absence of other complex correlated phenomena (e.g., phase separation [44,45], Jahn-Teller distortion [3,20], and charged ordered state in manganites [45], the extra incoherent band showing pseudogap in manganites [46] and Eu chalcogenides [47], and the electron polaron coupled replica bands [48] in Eu-chalcogenides) in $HgCr_2Se_4$ offers us the excellent opportunity to identify the key ingredients for the HSMT and CMR in half-metals. Our findings could be further applied to other half-metal systems such as manganites and Eu chalcogenides. Because the HSMT and CMR in these systems always appear in the same temperature regime near T_C [3,18–28], requiring additional turning knobs (e.g., doping [3,19–23,49], strain [3,19,20,50], etc.) to achieve both ferromagnetism and ideal E_F position.

Finally, we note that the observed band gap in FM state from ARPES and optical experiment contradicts the predicted Chern semimetal state [16] in $HgCr_2Se_4$. This is probably because of the relative overestimate of the spin-orbital coupling strength and the amplitude of band inversion.

In summary, we reveal a Lifshitz transition in n-$HgCr_2Se_4$ that results from exchange band splitting at a proper E_F. The observed electronic transition plays the dominant role of the HMST and CMR in n-$HgCr_2Se_4$. Our findings highlight that achieving both strong ferromagnetism and ideal E_F positions to fine-tune the electronic band structure are critical to the realization and application of the HMST and CMR among the spinel and other half-metal systems.

ACKNOWLEDGMENTS

We thank B. Fu very much for the stimulating discussions. This work was supported by a grant from Chinese Academy of Science-Shanghai Science Research Center (Grant No. CAS-SSRC-YH-2015-01). Y.L.C. acknowledges the support from an Engineering and Physical Sciences Research Council Platform grant (Grant No. EP/M020517/1) and Hefei Science Center Chinese Academy of Sciences (Grant No. 2015HSC-UE013). A.J.L. acknowledges the support from Scientific Support Group (SSG) Collaborative Postdoctoral Fellowship (P-1-06007) of the Department of Energy (DOE), Lawrence Berkeley National Laboratory (LBNL), and the Advanced Light Source (ALS). Z.K.L. acknowledges the support from the National Natural Science Foundation of China (Grant No. 12274298), the National Key R&D program of China (Grant No. 2022YFA1604400/03), and the double First-Class Initiative Fund of ShanghaiTech University. A.L.S. was supported by the U.S. DOE, Office of Basic Energy Sciences, under Contract No. DE-AC02-05CH11231.

[1] J. A. Sobota, Y. He, and Z.-X. Shen, Angle-resolved photoemission studies of quantum materials, Rev. Mod. Phys. **93**, 025006 (2021).

[2] M. Imada, A. Fujimori, and Y. Tokura, Metal-insulator transitions, Rev. Mod. Phys. **70**, 1039 (1998).

[3] A. P. Ramirez, Colossal magnetoresistance, J. Phys.: Condens. Matter **9**, 8171 (1997).

[4] N. Nagaosa, J. Sinova, S. Onoda, A. H. MacDonald, and N. P. Ong, Anomalous Hall effect, Rev. Mod. Phys. **82**, 1539 (2010).

[5] R. A. de Groot, F. M. Mueller, P. G. v. Engen, and K. H. J. Buschow, New Class of Materials: Half-Metallic Ferromagnets, Phys. Rev. Lett. **50**, 2024 (1983).

[6] M. A. Korotin, V. I. Anisimov, D. I. Khomskii, and G. A. Sawatzky, CrO_2: A Self-Doped Double Exchange Ferromagnet, Phys. Rev. Lett. **80**, 4305 (1998).

[7] Y. S. Dedkov, M. Fonine, C. Konig, U. Rudiger, G. Guntherodt, S. Senz, and D. Hesse, Room-temperature observation of high-spin polarization of epitaxial CrO_2(100) island films at the Fermi energy, Appl. Phys. Lett. **80**, 4181 (2002).

[8] R. Schiller and W. Nolting, Temperature-dependent band structure of bulk EuO, Solid State Commun. **118**, 173 (2001).

[9] Y. S. Dedkov, U. Rudiger, and G. Guntherodt, Evidence for the half-metallic ferromagnetic state of Fe_3O_4 by spin-resolved photoelectron spectroscopy, Phys. Rev. B **65**, 064417 (2002).

[10] J. I. Horikawa, T. Hamajima, F. Ogata, T. Kambara, and K. I. Gondaira, The spin polarised electronic band structure of chromium spinels: I. $CuCr_2S_4$, J. Phys. C: Solid State Phys. **15**, 2613 (1982).

[11] J. H. Park, E. Vescovo, H. J. Kim, C. Kwon, R. Ramesh, and T. Venkatesan, Direct evidence for a half-metallic ferromagnet, Nature (London) **392**, 794 (1998).

[12] T. Kise, T. Ogasawara, M. Ashida, Y. Tomioka, Y. Tokura, and M. Kuwata-Gonokami, Ultrafast Spin Dynamics and Critical Behavior in Half-Metallic Ferromagnet: Sr_2FeMoO_6, Phys. Rev. Lett. **85**, 1986 (2000).

[13] W. E. Pickett and J. S. Moodera, Half metallic magnets, Phys. Today **54**(5), 39 (2001).

[14] M. Jourdan, J. Minár, J. Braun, A. Kronenberg, S. Chadov, B. Balke, A. Gloskovskii, M. Kolbe, H. J. Elmers, G. Schönhense *et al.*, Direct observation of half-metallicity in the Heusler compound Co_2MnSi, Nat. Commun. **5**, 3974 (2014).

[15] H. Akinaga, T. Manago, and M. Shirai, Material design of half-metallic zinc-blende CrAs and the synthesis by molecular-beam epitaxy, Jpn. J. Appl. Phys. **39**, L1118 (2000).

[16] G. Xu, H. Weng, Z. Wang, X. Dai, and Z. Fang, Chern Semimetal and the Quantized Anomalous Hall Effect in $HgCr_2Se_4$, Phys. Rev. Lett. **107**, 186806 (2011).

[17] S. D. Guo and B. G. Liu, Density-functional-theory investigation of pressure induced semiconductor-metal transitions in the ferromagnetic semiconductor $HgCr_2Se_4$, J. Phys.: Condens. Matter **24**, 045502 (2012).

[18] T. Guan, C. Lin, C. Yang, Y. Shi, C. Ren, Y. Li, H. Weng, X. Dai, Z. Fang, S. Yan *et al.*, Evidence for Half-Metallicity in *n*-type $HgCr_2Se_4$, Phys. Rev. Lett. **115**, 087002 (2015).

[19] S. Jin, T. H. Tiefel, M. Mccormack, R. A. Fastnacht, R. Ramesh, and L. H. Chen, Thousandfold Change in Resistivity in Magnetoresistive La-Ca-Mn-O Films, Science **264**, 413 (1994).

[20] J. M. D. Coey, M. Viret, and S. von Molnar, Mixed-valence manganites, Adv. Phys. **48**, 167 (1999).

[21] M. W. Shafer and T. R. McGuire, Studies of Curie-Point Increases in EuO, J. Appl. Phys. **39**, 588 (1968).

[22] J. B. Torrance, M. W. Shafer, and T. R. McGuire, Bound Magnetic Polarons and the Insulator-Metal Transition in EuO, Phys. Rev. Lett. **29**, 1168 (1972).

[23] Y. Shapira, S. Foner, and T. B. Reed, EuO. I. Resistivity and Hall Effect in Fields up to 150 kOe, Phys. Rev. B **8**, 2299 (1973).

[24] A. P. Ramirez, R. J. Cava, and J. Krajewski, Colossal magnetoresistance in Cr-based chalcogenide spinels, Nature (London) **386**, 156 (1997).

[25] N. I. Solin, V. V. Ustinov, and S. V. Naumov, Colossal magnetoresistance of the inhomogeneous ferromagnetic semiconductor $HgCr_2Se_4$, Phys. Solid State **50**, 901 (2008).

[26] L. Goldstein, P. Gibart, and A. Selmi, Transport properties of the ferromagnetic semiconductor $HgCr_2Se_4$, J. Appl. Phys. **49**, 1474 (1978).

[27] C. J. Lin, Y. G. Shi, and Y. Q. Li, Analytical Descriptions of Magnetic Properties and Magnetoresistance in n-Type $HgCr_2Se_4$, Chin. Phys. Lett. **33**, 077501 (2016).

[28] M. Mitschek, T. J. Hicken, S. Yang, M. N. Wilson, F. L. Pratt, C. N. Wang, S. J. Blundell, Z. L. Li, Y. Q. Li, T. Lancaster *et al.*, Probing the magnetic polaron state in the ferromagnetic semiconductor $HgCr_2Se_4$ with muon-spin spectroscopy and resistance-fluctuation measurements, Phys. Rev. B **105**, 064404 (2022).

[29] J. P. Sun, Y. Y. Jiao, C. J. Yi, S. E. Dissanayake, M. Matsuda, Y. Uwatoko, Y. G. Shi, Y. Q. Li, Z. Fang, and J. G. Cheng, Magnetic-Competition-Induced Colossal Magnetoresistance in *n*-Type $HgCr_2Se_4$ under High Pressure, Phys. Rev. Lett. **123**, 047201 (2019).

[30] S. Yang, Z. Li, C. Lin, C. Yi, Y. Shi, D. Culcer, and Y. Li, Unconventional Temperature Dependence of the Anomalous Hall Effect in $HgCr_2Se_4$, Phys. Rev. Lett. **123**, 096601 (2019).

[31] C. Fang, M. J. Gilbert, X. Dai, and B. A. Bernevig, Multi-Weyl Topological Semimetals Stabilized by Point Group Symmetry, Phys. Rev. Lett. **108**, 266802 (2012).

[32] S. K. Jian and H. Yao, Correlated double-Weyl semimetals with Coulomb interactions: Possible applications to $HgCr_2Se_4$ and $SrSi_2$, Phys. Rev. B **92**, 045121 (2015).

[33] H. H. Lai, Correlation effects in double-Weyl semimetals, Phys. Rev. B **91**, 235131 (2015).

[34] W. Chen, K. Luo, L. Li, and O. Zilberberg, Proposal for Detecting Nodal-Line Semimetal Surface States with Resonant Spin-Flipped Reflection, Phys. Rev. Lett. **121**, 166802 (2018).

[35] H. W. Lehmann and F. P. Emmenegger, Crystal growth, semiconducting and optical properties of ferromagnetic $HgCr_2Se_4$, Solid State Commun. **7**, 965 (1969).

[36] T. Arai, Magnetoabsorption in Single-Crystal $HgCr_2Se_4$, J. Phys. Soc. Jpn. **34**, 68 (1973).

[37] A. N. Yaresko, Electronic band structure and exchange coupling constants in ACr_2X_4 spinels (A = Zn, Cd, Hg; X = O, S, Se), Phys. Rev. B **77**, 115106 (2008).

[38] K. M. G. V. G. Veselago, I. S. Kovaleva, and I. M. Yurin, Energy spectrum and transport properties of $HgCr_2Se_4$ single crystals, Zh. Eksp. Teor. Fiz. **86**, 1857 (1984).

[39] G. X. Gu *et al.*, (unpublished data).

[40] See Supplemental Material at http://link.aps.org/supplemental/10.1103/PhysRevB.107.195114 for details on the local inhomogeneity of doping level in *n*-$HgCr_2Se_4$; the stability of the potassium atoms adsorbed on *n*-$HgCr_2Se_4$; the electronic structure on the (001) surface from a heavily *n*-doped sample; the temperature dependence of the band structure of *n*-$HgCr_2Se_4$ without K doping; the splitting of the conduction and valence bands below T_C; and the critical role of the chemical nonstoichiometry in the HMST and CMR.

[41] A. Selmi, M. Heritier, and P. Gibartt, Spinel Magnetic Semiconductor $HgCr_2Se_4$, Prog. Crystal Growth Charact. **13**, 121 (1986).

[42] T. Rudolf, C. Kant, F. Mayr, J. Hemberger, V. Tsurkan, and A. Loidl, Spin-phonon coupling in antiferromagnetic chromium spinels, New J. Phys. **9**, 76 (2007).

[43] L. Li, L.-Q. Yan, Y. Shi, P. Lu, and Y. Sun, Evidence and evolution of magnetic polaron in $HgCr_2Se_4$ investigated by electron spin resonance, J. Phys.: Condens. Matter **30**, 255804 (2018).

[44] M. Fath, S. Freisem, A. A. Menovsky, Y. Tomioka, J. Aarts, and J. A. Mydosh, Spatially inhomogeneous metal-insulator transition in doped manganites, Science **285**, 1540 (1999).

[45] E. Dagotto, T. Hotta, and A. Moreo, Colossal magnetoresistant materials: The key role of phase separation, Phys. Rep. **344**, 1 (2001).

[46] D. E. Shai, A. J. Melville, J. W. Harter, E. J. Monkman, D. W. Shen, A. Schmehl, D. G. Schlom, and K. M. Shen, Temperature Dependence of the Electronic Structure and Fermi-Surface Reconstruction of $Eu_{1-x}Gd_xO$ through the Ferromagnetic Metal-Insulator Transition, Phys. Rev. Lett. **108**, 267003 (2012).

[47] E. J. Monkman, C. Adamo, J. A. Mundy, D. E. Shai, J. W. Harter, D. W. Shen, B. Burganov, D. A. Muller, D. G. Schlom, and K. M. Shen, Quantum many-body interactions in digital oxide superlattices, Nat. Mater. **11**, 855 (2012).

[48] J. M. Riley, F. Caruso, C. Verdi, L. B. Duffy, M. D. Watson, L. Bawden, K. Volckaert, G. van der Laan, T. Hesjedal, M. Hoesch *et al.*, Crossover from lattice to plasmonic polarons of a spin-polarised electron gas in ferromagnetic EuO, Nat. Commun. **9**, 2305 (2018).

[49] T. Miao, L. Deng, W. Yang, J. Ni, C. Zheng, J. Etheridge, S. Wang, H. Liu, H. Lin, Y. Yu *et al.*, Direct experimental evidence of physical origin of electronic phase separation in manganites, Proc. Natl. Acad. Sci. USA **117**, 7090 (2020).

[50] M. Baldini, T. Muramatsu, M. Sherafati, H. K. Mao, L. Malavasi, P. Postorino, S. Satpathy, and V. V. Struzhkin, Origin of colossal magnetoresistance in $LaMnO_3$ manganite, Proc. Natl. Acad. Sci. USA **112**, 10869 (2015).